Eur. Phys. J. B **17**, 3–6 (2000)

THE EUROPEAN PHYSICAL JOURNAL B

EDP Sciences

Rapid Note

Finite-temperature phase diagram of the Hubbard model

G. Migliorini[2,3] and A. Nihat Berker[1,2,3,a]

[1] Department of Physics, Istanbul Technical University, Maslak, Istanbul 80626, Turkey
[2] Department of Physics, Massachusetts Institute of Technology, Cambridge, Massachusetts 02139, USA
[3] Feza Gürsey Research Center for Basic Sciences, Çengelköy, Istanbul 81220, Turkey

Received 29 May 2000

Abstract. The finite-temperature phase diagram of the Hubbard model in $d = 3$ is obtained from renormalization-group analysis. It exhibits, around half filling, an antiferromagnetic phase and, between 30%–40% electron or hole doping from half filling, a new τ phase in which the electron hopping strength t asymptotically becomes infinite under repeated rescalings. Next to the τ phase, a first-order phase boundary with very narrow phase separation (less than 2% jump in electron density) occurs. At temperatures above the τ phase, an incommensurate spin modulation phase is indicated. In $d = 2$, we find that the Hubbard model has no phase transition at finite temperature.

PACS. 71.10.Fd Lattice fermion models (Hubbard model, etc.) – 74.25.Dw Superconductivity phase diagrams – 05.30.Fk Fermion systems and electron gas

The Hubbard model [1] is the bare-essentials realistic model of electronic conduction and is defined by the Hamiltonian

$$-\beta\mathcal{H} = -t \sum_{\langle ij\rangle,\sigma} \left(c^{\dagger}_{i\sigma} c_{j\sigma} + c^{\dagger}_{j\sigma} c_{i\sigma} \right) - U \sum_{i} n_{i\uparrow} n_{i\downarrow} + \mu \sum_{i} n_i, \qquad (1)$$

where $c^{\dagger}_{i\sigma}$ and $c_{i\sigma}$ are the electron creation and annihilation operators with spin $\sigma = \uparrow$ or $\downarrow$ at site i of a cubic lattice, $\langle ij\rangle$ indicates summation over all nearest-neighbor pairs of sites, and

$$n_{i\sigma} = c^{\dagger}_{i\sigma} c_{i\sigma} \text{ and } n_i = n_{i\uparrow} + n_{i\downarrow} \qquad (2)$$

are the electron number operators. The terms in the Hamiltonian of equation (1) are, respectively, the kinetic energy term, the on-site repulsion ($U > 0$) term, and the chemical potential term included in order to study the system over its entire density range from zero to two electrons per site.

Essentially no knowledge has existed even phenomenologically on the phase diagram of the Hubbard model as a function of (non-zero) temperature and (non-half-filling) electron density. Previous renormalization-group calculations have concentrated on studying the Hubbard model in lower dimensions, at zero-temperature, or at half-filling (*i.e.*, constrained to the electron density of one electron per site): The zero-temperature (ground-state) properties were successfully obtained in $d = 1, 2, 3$ [2]. In $d = 1$ at half filling, the thermodynamic properties were accurately calculated for finite temperatures [3]. In $d = 2$ at half filling, it was found that no phase transition as a function of temperature occurs [4,5]. This result was later extended to other fillings in $d = 2$ [6]. In $d = 3$ at half filling, an antiferromagnetic phase transition as a function of temperature was obtained [5]. One calculation done in $d = 3$ at finite temperature and arbitrary chemical potential [6] did not obtain the τ phase, the narrow phase separation, or the frozen spin modulation phase reported below.

In this research, we obtain a phase diagram for the Hubbard model in $d = 3$, for finite temperatures and for the full range of electron density, from an approximate renormalization-group calculation with flows in a 10-dimensional Hamiltonian space. This rich global phase diagram, in the variables of temperature, electron density, and on-site repulsion, exhibits, at and around half-filling, an antiferromagnetic phase completely due to electron hopping. This antiferromagnetic phase is unstable to at most 10% hole or electron doping from half filling. At 30–40% electron or hole doping from half filling, a new τ phase occurs with distinctive conduction property. In the neighborhood of the τ phase, a phase separation so narrow that the jump in electron density is less than 2% occurs. At temperatures above the τ phase, an incommensurate frozen spin modulation phase is indicated. In $d = 2$,

[a] e-mail: berkern@hidiv.cc.itu.edu.tr

we find that no phase separation or other phase transition occurs at *finite temperature* in the Hubbard model. This result agrees with previous renormalization-group calculations [4–6] and with quantum Monte Carlo calculations [7]. This behavior of the Hubbard model is in contrast to the phase transition in $d = 2$ in the closely related, but less realistic, tJ model of electronic conduction [8], also seen in the application of our method to the tJ model [9,10].

The renormalization-group transformation is formulated [9,10] by first considering a $d = 1$ system. An exact renormalization-group transformation can be formally written,

$$\langle u_1 u_3 u_5 ... \mid \mathrm{e}^{-\beta' \mathcal{H}'} \mid v_1 v_3 v_5 ... \rangle = \sum_{w_2 w_4 w_6 ...} \langle u_1 w_2 u_3 w_4 u_5 w_6 ... \mid \mathrm{e}^{-\beta \mathcal{H}} \mid v_1 w_2 v_3 w_4 v_5 w_6 ... \rangle, \tag{3}$$

where u_1, w_2, v_3, etc. represent the single-site states. Primes indicate the renormalized system. The transformation given in equation (3) conserves the partition function, $Z = Z'$, but cannot be implemented due to the noncommutativity of the operators in the Hamiltonian. An approximation is used:

$$\begin{aligned} \mathrm{Tr}_{\mathrm{even}} \exp(-\beta \mathcal{H}) &= \mathrm{Tr}_{\mathrm{even}} \\ &\times \exp\left(\sum_i^{\mathrm{even}} -\beta \mathcal{H}(i-1,i) - \beta \mathcal{H}(i,i+1) \right) \\ &\simeq \prod_i^{\mathrm{even}} \mathrm{Tr}_{w_i} \exp\left(-\beta \mathcal{H}(i-1,i) - \beta \mathcal{H}(i,i+1) \right) \\ &= \prod_i^{\mathrm{even}} \exp\left(-\beta' \mathcal{H}'(i-1,i+1) \right) \\ &\simeq \exp\left(\sum_i^{\mathrm{even}} -\beta' \mathcal{H}'(i-1,i+1) \right) \\ &= \exp(-\beta' \mathcal{H}'), \end{aligned} \tag{4}$$

where $\mathrm{Tr}_{\mathrm{even}}$ means a trace taken only over the even sites, and

$$\begin{aligned} -\beta \mathcal{H}(i,j) = &-t \left(c_{i\sigma}^\dagger c_{j\sigma} + c_{j\sigma}^\dagger c_{i\sigma} \right) \\ &- (U/2d) \sum_i \left(n_{i\uparrow} n_{i\downarrow} + n_{j\uparrow} n_{j\downarrow} \right) \\ &+ (\mu/2d) \sum_i \left(n_i + n_j \right). \end{aligned} \tag{5}$$

Thus, the approximation consists in neglecting the commutation relations beyond segments of three consecutive unrenormalized sites. This approximation is effected twice ($\simeq$) in equation (4), in opposing directions, hopefully with compensatory effect. The crux of the calculation is extracted from the third step in equation (4),

$$\mathrm{Tr}_{w_2} \mathrm{e}^{-\beta \mathcal{H}(1,2) - \beta \mathcal{H}(2,3)} = \mathrm{e}^{-\beta' \mathcal{H}'(1,3)} \ . \tag{6}$$

When written in terms of three-site (on the left) and two-site (on the right) matrix elements, this equation amounts to contracting a 64×64 matrix into a 16×16 matrix. This operation is facilitated by block diagonalization of the matrices, using the conservations of particles, total spin magnitude, total spin z-component, and parity, so that the largest blocks are 4×4 and 2×2 for the unrenormalized and renormalized systems, respectively. Thus, a renormalized Hamiltonian $-\beta' \mathcal{H}'$ is extracted. The closed form of $-\beta' \mathcal{H}'$ is more general than equation (1), namely

$$\begin{aligned} -\beta \mathcal{H} = &- \sum_{\langle ij \rangle, \sigma} \left[t_0 h_{i-\sigma} h_{j-\sigma} + t_1 \left(n_{i-\sigma} h_{j-\sigma} + h_{i-\sigma} n_{j-\sigma} \right) \right. \\ &\left. + t_2 n_{i-\sigma} n_{j-\sigma} \right] \left(c_{i\sigma}^\dagger c_{j\sigma} + c_{j\sigma}^\dagger c_{i\sigma} \right) \\ &- t_x \sum_{\langle ij \rangle} \left(c_{i\uparrow}^\dagger c_{j\uparrow} c_{i\downarrow}^\dagger c_{j\downarrow} + c_{j\uparrow}^\dagger c_{i\uparrow} c_{j\downarrow}^\dagger c_{i\downarrow} \right) \\ &- U \sum_i n_{i\uparrow} n_{i\downarrow} + \mu \sum_i n_i \\ &+ \sum_{\langle ij \rangle} \left[J \mathbf{s}_i \cdot \mathbf{s}_j + V_2 n_i n_j + V_3 \left(n_{i\uparrow} n_{i\downarrow} n_j + n_i n_{j\uparrow} n_{j\downarrow} \right) \right. \\ &\left. + V_4 n_{i\uparrow} n_{i\downarrow} n_{j\uparrow} n_{j\downarrow} \right], \end{aligned} \tag{7}$$

where the hole operator is $h_{i\sigma} \equiv 1 - n_{i\sigma}$ and the electron spin operator at site i is

$$\mathbf{s}_i = \sum_{\sigma, \sigma'} c_{i\sigma}^\dagger \mathbf{s}_{\sigma\sigma'} c_{i\sigma'} \ , \tag{8}$$

where $\mathbf{s}_{\sigma\sigma'}$ is the vector of Pauli spin matrices. The four hopping terms in the flow Hamiltonian (Eq. (7)) correspond to one electron hopping with or without the opposite spin electron present at the initial and final sites (two of these processes are related by hermitivity and therefore have the same hopping strength t_1) and to two electrons simultaneously hopping from one site to a neighboring site. These four processes can be called vacancy hopping (t_0), pair breaking (t_1), pair hopping (t_2), and vacancy-pair interchange (t_x). For

$$t_0 = t_1 = t_2 \ , \quad t_x = J = V_2 = V_3 = V_4 = 0 \ , \tag{9}$$

the flow Hamiltonian (Eq. (7)) reduces to the Hubbard Hamiltonian (Eq. (1)). Thus, equations (9) are the initial conditions of our renormalization-group flows. However, in general, the hopping strengths renormalize differently and the new interactions are generated under rescaling, so that the renormalization-group flows are in the 10-dimensional, $\mathbf{K} = (t_0, t_1, t_2, t_x, U, \mu, J, V_2, V_3, V_4)$, Hamiltonian space.

The transformation is implemented in $d > 1$ by using the Migdal-Kadanoff procedure, so that $\mathbf{K}' = (b^{d-1}/f)\mathbf{R}(f\mathbf{K})$ where $b = 2$ is the length-rescaling factor, the function $\mathbf{R}$ is the contraction process specified in the previous paragraph, and f is an arbitrary bond-moving factor, set to yield the correct transition temperature of the Ising model ($f = 1.2279$ and 1.4024 in $d = 3$ and 2). This renormalization-group transformation yields known information about quantum systems, such as, in $d = 1$,

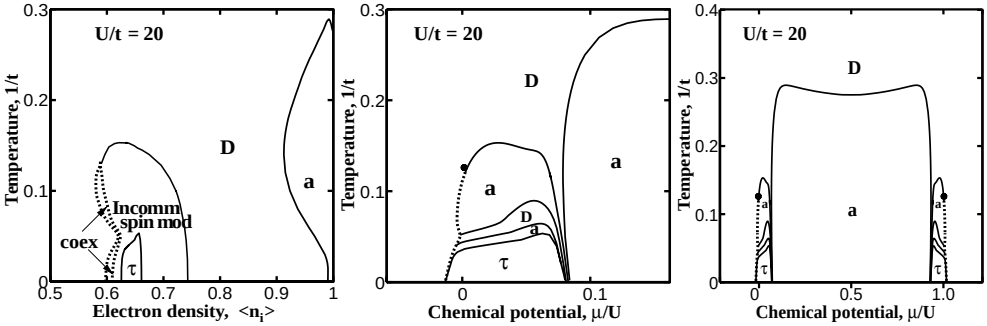

Fig. 1. Calculated phase diagram of the $d = 3$ Hubbard model for $U/t = 20$. First- and second-order phase boundaries are shown with dotted and full curves, respectively. The right panel shows the full phase diagram in temperature *versus* chemical potential, which is symmetric about $\mu/U = 0.5$. The middle panel shows a detailed view. The left panel shows the same phase diagram as the middle panel, but in temperature *versus* electron density. Antiferromagnetic [a], disordered [D], and τ phases are seen. In the τ phases, the hopping strength t_0 or t_2 renormalizes to infinity, for hole or electron doping respectively. Above the τ phase, a sequence of antiferromagnetic and disordered phases (Fig. 1 (center panel)) is interpreted as an incommensurate spin modulation phase (Fig. 1 (left panel)). As seen in (left), the first-order phase boundary has a very narrow coexistence region.

the absence finite-temperature phase transitions; in $d = 2$, a conventional phase transition for the Ising model, a Kosterlitz-Thouless transition for the XY model [11,12], no phase transition for the Heisenberg model; in $d = 3$, ferromagnetic and antiferromagnetic phase transitions for the Heisenberg model, the antiferromagnetic transition occurring at a 22% higher temperature than the ferromagnetic transition, a purely quantum mechanical effect [13]. The 10-dimensional renormalization-group flows also conserve the particle-hole symmetry, given by the map:

$$\begin{aligned} &\overline{t}_0 = t_2\ ,\ \ \overline{t}_1 = t_1\ ,\ \ \overline{t}_2 = t_0\ ,\ \ \overline{t}_x = t_x\ ,\ \ \overline{J} = J, \\ &\overline{\mu} = -\mu + U - 4dV_2 - 6dV_3 - 2dV_4,\ \overline{U} = U - 4dV_3 - 2dV_4, \\ &\overline{V}_2 = V_2 + 2V_3 + V_4\ ,\ \ \overline{V}_3 = -V_3 - V_4\ ,\ \ \overline{V}_4 = V_4. \quad (10) \end{aligned}$$

The global analysis of the renormalization-group flows yields the phase diagram of the system. Within renormalization-group theory, each thermodynamic phase is identified as the basin of attraction, within renormalization-group flows, of a completely stable characteristic fixed point (sink). Analysis of the (at least singly) unstable fixed points attracting the points in-between the thermodynamic phases yields the properties of the first- or second-order phase transitions. For any given temperature and chemical potential, the electron density can be calculated by summation along the entire renormalization-group trajectory that originates at the given temperature and chemical potential [9]. Thus, once a phase diagram is obtained in temperature *versus* chemical potential, it can also be obtained in temperature *versus* electron density simply by calculating the electron density at each phase boundary point of the temperature and chemical potential phase diagram. This was done in our work and sets of corresponding phase diagrams are exhibited below. We have thus obtained the global phase diagram of Hubbard model, presented here in Figures 1–3, where first- and second-order phase boundaries are respectively shown by dotted and full curves. The particle-hole symmetry (Eq. (10)) dictates that the Hubbard model (Eq. (1)) phase diagrams be symmetric about $\mu/U = 0.5$, which is seen in all of our results.

Figures 1 are for $U/t = 20$. In Figure 1, the right panel shows the full phase diagram in temperature *versus* chemical potential. The middle panel shows the details in temperature *versus* chemical potential. The left panel shows the same phase diagram as the middle panel, but in temperature *versus* electron density, which is calculated as explained above. It is seen that an antiferromagnetic phase (marked as a in the figures) occurs at and around half-filling, purely due to electron hopping, since the Hubbard Hamiltonian (Eq. (1)) does not contain an explicit antiferromagnetic coupling. In fact, we traced the occurrence of this antiferromagnetic phase to the non-zero value of the pair-breaking strength t_1. This antiferromagnetic phase is unstable to at most 10% hole or electron doping from half filling. Between 30 to 40% hole or electron doping, a τ phase occurs in which the vacancy hopping strength t_0 or the pair hopping strength t_2 (see Eq. (7)), respectively, renormalizes to infinity under repeated renormalization-group transformations. Thus, for hole doping, under repeated renormalization-group transformations, $t_0 \to \infty, J/t_0 = 2, V_2/t_0 = 3/2, \mu/t_0 = 6, t_{i\neq 0} = 0, U \to \infty, t_i/U = 0, V_i/U = 0$. Symmetrically, for electron doping, the overbarred variables of equation (10) have this behavior. In all other regions of the phase diagram, all hopping strengths renormalize to zero under repeated renormalization-group transformations. Near the τ phase, a first-order phase transition (dotted curves) occurs, seen as a single curve in Figure 1 (center) in terms of electron chemical potential and opening up into a coexistence region in Figure 1 (left) in terms of electron density. The latter shows the distinctive feature of this first-order transition, namely that it involves a very narrow phase separation, *e.g.*, a discontinuity in electron density of less than 2%. This is similar to what is seen experimentally [14] in lanthanide compounds, which are physical realizations of an electronic conduction system. At temperatures above the τ phase, a sequence of antiferromagnetic and disordered phases

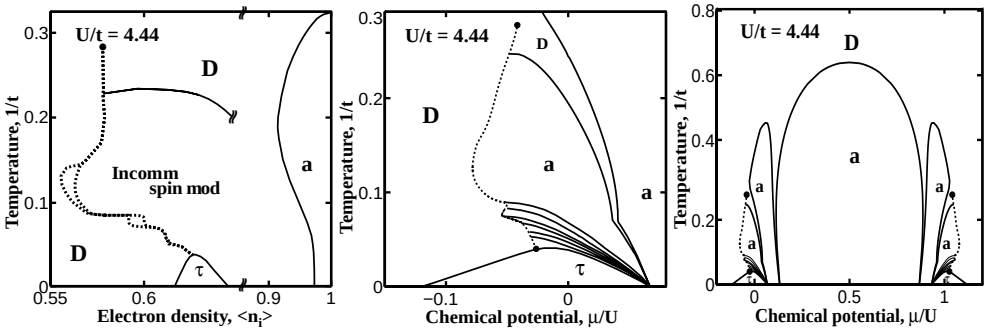

Fig. 2. Calculated phase diagram of the $d = 3$ Hubbard model for $U/t = 4.44$.

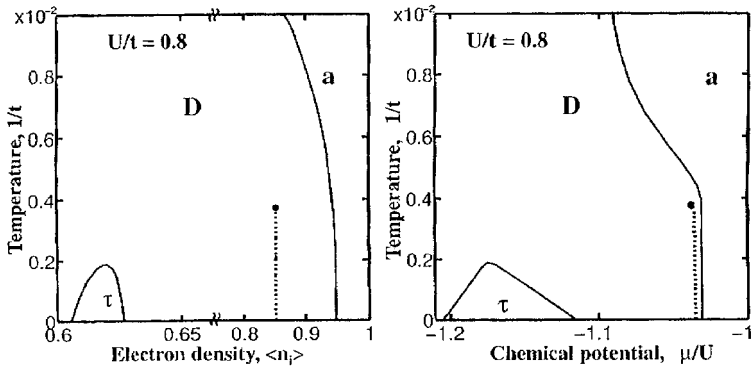

Fig. 3. Calculated phase diagram of the $d = 3$ Hubbard model for $U/t = 0.8$.

is seen, at many temperature scales (Figs. 1, 2 (center)). We interpret this as the presence of an incommensurate spin modulation phase, with a temperature- and (less strongly, by the alignment of the sequencing) density-dependent periodicity. Our renormalization-group transformation, with a commensurate rescaling factor and a built-in approximation, acts as a spurious substrate potential which, at small incommensuration, registers the incommensurate phase and, at large incommensuration, disorders it. This is also apparent in incommensurate phases of spin systems, as seen for example in Figure 4 of reference [15]. The incommensurate phase that we thus deduce is indicated in Figures 1, 2 (left). Finally, in the disordered (D) phase, all intersite couplings and hopping strengths renormalize to zero under repeated renormalization-group transformations. The features described above were also seen in the simpler, less realistic, tJ model [9,10].

As U/t is decreased, the first-order phase boundary moves with respect to the τ phase. It is seen that, for $U/t = 4.44$ (Figs. 2), it actually abuts the boundary of the τ phase and, for $U/t = 0.8$ (Figs. 3), it is on the other side of the τ phase.

We have thus calculated a finite-temperature phase diagram for the $d = 3$ Hubbard model, which has yielded rich phase transition phenomena. We have also repeated the same calculation for $d = 2$. We find that, *at finite-temperature*, no phase separation or other phase transition occurs for the Hubbard model (Eq. (1)) in $d = 2$. This result agrees with previous renormalization-group calculations [4–6] and with quantum Monte Carlo calculations [7]. By contrast, our renormalization-group method has also been applied to the tJ model, where a phase separation bounded by a finite temperature critical line is found for $t/J \leq 0.25$ [9,10].

This research was supported by the Italian Istituto Nazionale di Fisica Nucleare (INFN), US Department of Energy under Grant No. DE-FG02-92ER45473, and by the Scientific and Technical Research Council of Turkey (TÜBITAK). GM gratefully acknowledges the hospitality of the Feza Gürsey Research Center for Basic Sciences.

References

1. J. Hubbard, Proc. R. Soc. A **276**, 238 (1963); **277**, 237 (1964); **281**, 401 (1964).
2. J.E. Hirsch, Phys. Rev. B **11**, 5259 (1980).
3. C. Vanderzande, A.L. Stella, J. Phys. C **17**, 2075 (1984).
4. C. Vanderzande, J. Phys. A **18**, 889 (1985).
5. S.A. Cannas, F.A. Tamarit, C. Tsallis, Solid State Commun. **78**, 685 (1991).
6. S.A. Cannas, C. Tsallis, Z. Phys. B **89**, 195 (1992).
7. A.C. Cosentini, M. Capone, L. Guidoni, G. Bachelet, Phys. Rev. B **58**, 18235 (1998).
8. S.A. Kivelson, V.J. Emery, H.Q. Lin, Phys. Rev. B **42**, 6523 (1990).
9. A. Falicov, A.N. Berker, Phys. Rev. B **51**, 12458 (1995).
10. A. Falicov, A.N. Berker, Turk. J. Phys. **19**, 127 (1995).
11. M. Suzuki, H. Takano, Phys. Lett. A **69**, 426 (1979).
12. H. Takano, M. Suzuki, J. Stat. Phys. **26**, 635 (1981).
13. G.S. Rushbrooke, P.J. Wood, Mol. Phys. **6**, 409 (1963), calculate this effect as 14% from series expansion.
14. F.C. Chou, D.C. Johnston, Phys. Rev. B **54**, 572 (1996).
15. M. Aydin, M.C. Yalabik, J. Phys. A **22**, 3981 (1989).